Optics Letters

Plasmonic analogue of geometric diodes realizing asymmetric optical transmission

ZE ZHENG,[1,2] MOHAMED ELKABBASH,[3,5] JIHUA ZHANG,[3,4] AND CHUNLEI GUO[1,3,*]

[1]GPL, Changchun Institute of Optics, Fine Mechanics and Physics, Chinese Academy of Science, Changchun130033, China
[2]University of Chinese Academy of Science, Beijing 100039, China
[3]The Institute of Optics, University of Rochester, New York, New York 14627, USA
[4]Present address: Nonlinear Physics Centre, Research School of Physics, The Australian National University, Canberra, ACT 2601, Australia
[5]e-mail: melkabba@ur.rochester.edu
*Corresponding author: guo@optics.rochester.edu

Received 15 May 2020; revised 14 June 2020; accepted 15 June 2020; posted 16 June 2020 (Doc. ID 397601); published 10 July 2020

Geometric diodes represent a relatively new class of diodes used in rectennas that rely on the asymmetry of a conducting thin film. Here, we numerically investigate a plasmonic analogue of geometric diodes to realize nanoscale optical asymmetric transmission. The device operates based on spatial symmetry breaking that relies on a unique property of surface plasmon polaritons (SPPs), namely, adiabatic nanofocusing. We show that the structure can realize on-chip asymmetric electromagnetic transmission with a total dimension of ∼2 µm × 6 µm. We demonstrate a signal contrast of 0.7 and an asymmetric optical transmission ratio of 4.77 dB. We investigate the origin of the asymmetric transmission and show that it is due mainly to asymmetric out-coupling of SPPs to far-field photons. We highlight the role of evanescent field coupling of SPPs in undermining the asymmetric transmission efficiency and show that by adjusting the plasmonic waveguide dimensions, a signal contrast of 0.94 and an asymmetric optical transmission ratio of 5.18 dB can be obtained. Our work presents a new paradigm for on-chip nanoscale asymmetric optical transmission utilizing the unique properties of SPPs.

https://doi.org/10.1364/OL.397601

The ability to control and manipulate electromagnetic waves at the nanoscale is the hallmark of modern nanophotonics. One of the major themes is to realize on-chip and nanoscale devices with functionalities that replace bulky optical elements. The goal is to create nano-photonic circuits that combine the advantages of electronics and photonics [1]. The developments of metatronics [2], plasmonic circuits [1], and metasurfaces [3] are testimonies to the major role of photonics in future devices.

Of particular interest are optical isolators and diodes, which are crucial to regulate signal propagation and minimize potentially harmful reflection of induced scattering, allowing the separation of forward and backward signal flow [4]. Optical isolation, in general, requires systems that break Lorenz reciprocity and commonly rely on the Faraday rotation effect [5]. However, these isolators require external polarizers or analyzers and are bulky. Recent advances in nanophotonics led to the demonstration of Faraday-like rotation using metasurfaces [6], isolation based on temporally modulated refractive index [7], and isolation based on nonlinear electromagnetic response of materials [8]. On the other hand, on-chip asymmetric transmission has also received significant research interest for its potential applications in integrated photonic systems for communications and information processing [9]. Asymmetric transmission is a reciprocal effect characterized by a strong contrast between forward and reverse transmissions. Asymmetric transmission relies on structures that break the spatial inversion symmetry and has been realized using hyperbolic metamaterials with double-sided asymmetric gratings [9], phase-gradient metasurfaces [10], spatially asymmetric gratings [11,12], and photonic crystals [13].

Optical isolation and asymmetric transmission are functionally similar to diodes in electronics. Diodes are two-terminal electronic components that conduct current mainly in the forward direction, while blocking current in the reverse direction, i.e., enjoying asymmetric conductance. An important class of electronic diodes is geometric diodes, which are commonly used in rectennas [14]. The working principle of geometric diodes is shown schematically in Fig. 1(a). A geometric diode is a spatially asymmetric device that operates in the ballistic conduction regime and enables dissimilar current for forward and reverse biased voltages. In the ballistic conduction regime, electrons scatter only upon collision with the walls of the device. The device consists of a patterned conductive thin film where the size of the constriction is on the order of the mean free path of the charge carriers in the material [14]. Using the design shown in Fig. 1(a), charge carriers reflect at the boundaries of the device. The vertical edge of the rectangular metallic slab blocks charge carriers upon scattering from the metallic strip.

In this Letter, we numerically demonstrate a plasmonic analogue to geometric diodes. We show that surface plasmon polaritons (SPPs) propagating in a metallic waveguide with a design similar to a geometric diode experience significant asymmetric transmission. We investigate the origin of the observed asymmetric transmission and methods to optimize the asymmetry, which provides us with a signal contrast of ∼0.94

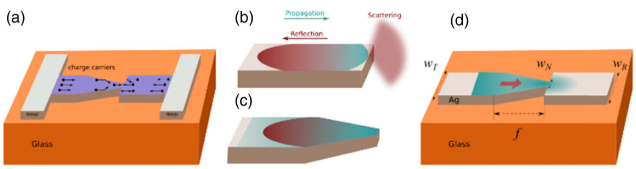

Fig. 1. (a) Geometric diodes operation principle. Black dots represent electrons with ballistic motion, and the arrows show the effect of scattering and reflection from the conductor edges. For the tapered conductor, ballistic electrons reflect but can still be focused on an aperture, as their motion is dictated by the DC electric field. (b) SPPs propagating in the forward direction (dark green) exist only at the metal–dielectric interface. When they interact with the metallic waveguide edge, SPPs either reflect (wine) or scatter into a photon. (c) For a tapered metallic waveguide, SPPs can be focused to dimensions significantly below the diffraction limit without scattering or reflection from the waveguide edge. If, however, SPPs suddenly encounter the end of the tapered waveguide, they will reflect and scatter as well. (d) Schematic of the plasmonic analogue of geometric diodes featuring a tapered waveguide and a rectangular waveguide.

for round-trip transmission. Finally, we show that our system exhibits plasmonic isolation by demonstrating asymmetric mode-to-mode conversion.

The electron–metallic conductor interaction in geometric diodes shares similar propagation properties with SPPs. SPPs are electromagnetic waves that propagate at a metal–dielectric interface. As a surface wave, SPPs evanescently decay in the metallic substrate, due to the negative permittivity of metals, and dielectric superstrate, due to total internal reflection. SPPs, however, can couple/outcouple to a propagating electromagnetic wave if a phase coupling mechanism is involved, e.g., through prism coupling, grating coupling, or edge/scatterer coupling. Consequently, SPPs propagating in a rectangular metallic slab will either reflect or scatter off the slab's edges to a propagating electromagnetic wave (photon) [Fig. 1(b)]. Moreover, tapering the waveguide can focus SPPs. SPPs can be focused well below the diffraction limit, as more energy can be stored in the electron motion [Fig. 1(c)]. The SPP mode index increases when focused, leading to slower SPP propagation. The index mismatch can reflect the SPP. However, reflection can be minimized through adiabatic nanofocusing where the waveguide is tapered such that the variation in the SPP mode index is negligible over the SPP wavelength [15]. Accordingly, using a tapered metallic substrate, an SPP wave can be focused onto a narrow aperture/neck without significantly scattering from the edges.

The proposed plasmonic asymmetric transmission device is shown in Fig. 1(d). The device consists of a tapered silver (Ag) plasmonic waveguide connected to a rectangular Ag waveguide through a neck. In the forward direction, SPPs are launched and adiabatically focused on an aperture (so-called neck). On the other hand, SPPs propagating in the reverse direction mainly scatter or reflect from the edges, while only a small portion is transmitted through the neck. The relevant design dimensions are the widths of the tapered and rectangular waveguides, w_T and w_R, respectively; the length of the tapered waveguide, i.e., focus length, f; and the neck's width, w_N. Note that the width and length of the tapered waveguide determine the tapering angle. Simulations were performed using the commercially available finite-difference time-domain software from Lumerical. The Ag film thickness is 500 nm on a glass substrate, the permittivity of sliver is calculated following the Drude model, and the SPPs are excited by a mode source. Scattering is calculated by integrating the power detected by monitors surrounding the scattered field region. The SPP reflection is obtained using a monitor placed 10 nm behind the mode source.

Figure 2(a) shows the calculated transmission (T) in the forward and reverse directions. The design dimensions are $w_T = w_R = 2000$ nm, $f = 5000$ nm, and $w_N = 50$ nm. Maximum transmission difference (ΔT) is obtained between 600 nm and 750 nm and is ~ 0.2. The signal contrast defined as $(T_{\text{Forward}} - T_{\text{Reverse}})/T_{\text{Forward}}$ is ~ 0.7 at a wavelength $\lambda = 700$ nm, and an asymmetric optical transmission ratio defined as $10\,\text{Log}_{10}[T_{\text{Forward}}/T_{\text{Reverse}}]$ is $\sim$4.77 dB. The corresponding electric field distributions of the forward and backward propagations at $\lambda = 750$ nm are shown in Fig. 2(b) and Fig. 2(c), respectively. We note the following observations: (i) in the forward direction, the SPP field intensity increases significantly due to adiabatic nanofocusing; (ii) in the reverse direction, evanescent wave coupling from the rectangular guide to the tapered guide takes place, i.e., the evanescent field of the SPP at the edge of the rectangular guide experiences frustrated total internal reflection where it converts to a propagating SPP as it couples to another plasmonic waveguide [16].

To fully understand the origin of the observed asymmetric transmission, we calculate the scattering (S), reflection (R), and absorption (A) for forward and reverse propagations, as shown in Fig. 2(d), Fig. 2(e), and Fig. 2(f), respectively. We note that $T = 1 - S - R - A$, i.e., we can fully understand the asymmetry in transmission by analyzing S, R, and A. Scattering here refers to the SPPs scattered into a far-field mode propagating in free space (radiation), which was calculated by engulfing the plasmonic waveguide with plane monitors to measure the radiated intensity. Scattering is significantly higher in the reverse direction compared to forward direction, as the SPPs outcouple and radiate after scattering off the edges. On the other hand, the calculated reflection and absorption are higher

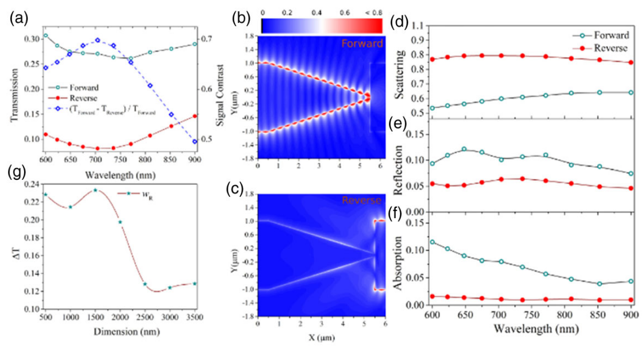

Fig. 2. (a) Calculated transmission of SPPs in the forward (green open circles) and reverse (red circles) direction. The corresponding signal contrast reaches a peak $\sim$0.7 at 700 nm. The calculated electric field magnitude $|E|$ in the (b) forward and (c) reverse directions. Note that in the forward direction, SPPs are focused onto the aperture, while in the reverse direction, SPPs scatter off the rectangular waveguide edges. Also note the evanescent field coupling between the rectangular and tapered waveguides in the reverse direction. Calculated (d) scattering to photons, (e) SPP reflection, and (f) absorption. (g) Transmission difference between forward and reverse directions as a function of the rectangular waveguide width w_R.

for the forward versus reverse propagation directions. At the aperture, the nanofocused SPP experiences a strong reflection due to the sudden change in the index contrast. Additionally, the absorption in the forward direction is higher, as the stronger field confinement imposed by the tapered waveguide increases the optical losses in the metal.

The calculated transmission in the reverse direction, however, is significantly higher than expected since the ratio of the aperture to the rectangular waveguide width is ∼0.025, i.e., one expects the transmission to be ∼0.025. The higher transmission is due to the evanescent field coupling (tunneling) that we discussed earlier, which circumvents the aperture. Moreover, the evanescent field coupling allows the field to "tunnel" to various positions on the tapered waveguide, which decreases the additional absorption and reflection associated with SPP propagation in the tapered waveguide.

A method that can limit the evanescent field coupling would increase the signal contrast significantly. We mitigate the evanescent field coupling by varying the width of the rectangular guide w_R while keeping $w_T = 2000$ nm. Our purpose is to find the ideal w_R where the ratio of the aperture width to w_R is minimized while limiting the evanescent coupling to points further along the tapered waveguide. Figure 2(g) shows the calculated T at $\lambda = 750$ nm as we vary w_R while maintaining $w = 2000$ nm. For all $w_R < w_T$, ΔT experiences ∼20% increase. Optimal ΔT is obtained for $w_R = 1500$ nm. In other words, by decreasing w_R, evanescent field coupling is limited to regions in the tapered waveguide with narrower width and higher absorption.

Although our system is fully reciprocal from an electromagnetic point of view [5], we argue that it performs the function of an isolator if we consider only SPPs, i.e., the mode-to-mode transmission coefficient is asymmetric only when considering the electromagnetic field propagating as an SPP. For optical isolators, mode-to-mode conversion must be asymmetric, i.e., the transmission of mode A to mode B in the forward direction (T_{AB}) is not equal to the transmission of mode B to mode A in the reverse direction (T_{BA}) [17,18]. In our case, due to the ability of the structure to outcouple SPPs to far-field radiation, asymmetric plasmonic mode-to-mode conversion is possible. To test this claim, we investigate two modes supported by our plasmonic waveguides. Figures 3(a) and 3(b) show the field distribution of mode A and mode B; the effective refractive indices of mode A and of mode B are 0.97 and 1.02, respectively. Figure 3(c) shows that the calculated $T_{AB} \neq T_{BA}$, proving that our system acts as a plasmonic isolator. Certainly, our device serves the purpose of isolators, i.e., even if the properties of the scattered SPPs are unknown, the signal in the reverse direction is significantly diminished [18]. To test this claim, we calculate the round-trip transmission, i.e., transmission assuming a signal that is input from the tapered waveguide in the forward direction and is then reflected backwards and collected at the input. The results are shown in Fig. 3(d) where the round-trip transmission is significantly lower than either forward or reverse transmissions shown previously in Fig. 2(a). Moreover, the signal contrast now approaches unity at ∼600 nm. We stress that our proposed device is fully reciprocal if we consider the totality of the input and output electromagnetic field and does not break Lorentz non-reciprocity.

In conclusion, we proposed a plasmonic analogue of geometric diodes that exhibits strong asymmetric transmission. The asymmetry is imposed by creating a constriction where SPPs are adiabatically focused on an aperture in the forward direction and scatter off the waveguide edge in the reverse direction. The device exhibits plasmonic isolation, as it enables the mode-to-mode transmission to be asymmetric.

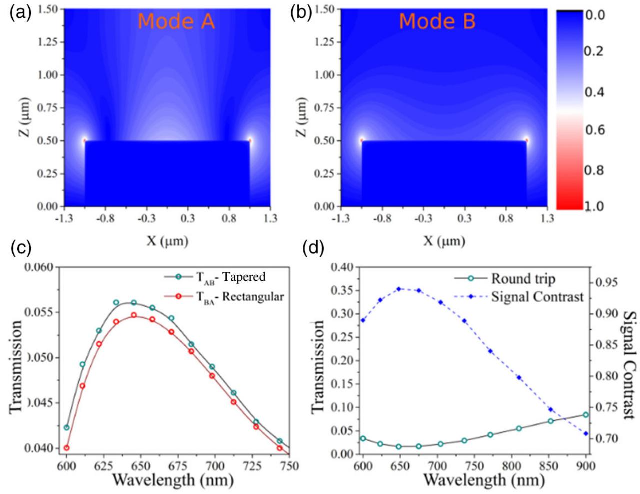

Fig. 3. Calculated electric field distributions of (a) mode A and (b) mode B. (c) Calculated mode-to-mode transmission showing a proof for "plasmonic" isolation. (d) To determine the practicality of the geometric plasmonic diode, we calculate the round-trip transmission and round-trip signal contrast.

Funding. K. C. Wong Education Foundation (GJTD-2018-08); National Natural Science Foundation of China (11774340, 91750205); National Science Foundation.

Disclosures. The authors declare no conflicts of interest.

REFERENCES

1. T. J. Davis, D. E. Gómez, and A. Roberts, Nanophotonics **6**, 543 (2016).
2. C. D. Giovampaola and N. Engheta, Nat. Mater. **13**, 1115 (2014).
3. J. Zhang, M. ElKabbash, R. Wei, S. C. Singh, B. Lam, and C. Guo, Light Sci. Appl. **8**, 53 (2019).
4. Z. Wang and S. Fan, Opt. Lett. **30**, 1989 (2005).
5. V. Asadchy, M. S. Mirmoosa, A. Díaz-Rubio, S. Fan, and S. A. Tretyakov, "Tutorial on electromagnetic nonreciprocity and its origins," arXiv preprint arXiv:2001.04848 (2020).
6. A. M. Mahmoud, A. R. Davoyan, and N. Engheta, Nat. Commun. **6**, 8359 (2015).
7. Z. Yu and S. Fan, Nat. Photonics **3**, 91 (2009).
8. D. L. Sounas and A. Alù, Phys. Rev. B **97**, 115431 (2018).
9. T. Xu and H. J. Lezec, Nat. Commun. **5**, 4141 (2014).
10. Z. Li, M.-H. Kim, C. Wang, Z. Han, S. Shrestha, A. C. Overvig, M. Lu, A. Stein, A. M. Agarwal, M. Lončar, and N. Yu, Nat. Nanotechnol. **12**, 675 (2017).
11. S. Cakmakyapan, H. Caglayan, A. E. Serebryannikov, and E. Ozbay, Appl. Phys. Lett. **98**, 051103 (2011).
12. S. Cakmakyapan, A. E. Serebryannikov, H. Caglayan, and E. Ozbay, Opt. Lett. **35**, 2597 (2010).
13. C. Wang, X.-L. Zhong, and Z.-Y. Li, Sci. Rep. **2**, 674 (2012).
14. Z. Zhu, S. Joshi, S. Grover, and G. Moddel, *Rectenna Solar Cells* (Springer, 2013), pp. 209–227.
15. M. I. Stockman, Phys. Rev. Lett. **93**, 137404 (2004).
16. S. Sidorenko and O. J. F. Martin, Opt. Express **15**, 6380 (2007).

17. D. Jalas, A. Petrov, M. Eich, W. Freude, S. Fan, Z. Yu, R. Baets, M. Popović, A. Melloni, J. D. Joannopoulos, M. Vanwolleghem, C. R. Doerr, and H. Renner, Nat. Photonics **7**, 579 (2013).
18. S. Fan, R. Baets, A. Petrov, Z. Yu, J. D. Joannopoulos, W. Freude, A. Melloni, M. Popović, M. Vanwolleghem, D. Jalas, M. Eich, M. Krause, H. Renner, E. Brinkmeyer, and C. R. Doerr, Science **335**, 38 (2012).